Fingerprint Compression Using Contourlet Transform with Modified SPIHT Algorithm

R. Sudhakar, R. Karthiga, and S. Jayaraman

Abstract—Large volumes of fingerprints are collected and stored every day in a wide range of applications, including forensics, access control etc., and is evident from the database of Federal Bureau of Investigation (FBI) which contains more than 70 million finger prints. Wavelet based Algorithms for image compression are the most successful, which result in high compression ratios compared to other compression techniques. Even though wavelet bases are providing good compression ratios, they are not optimal for representing images consisting of different regions of smoothly varying grey-values, separated by smooth boundaries. This issue is addressed by the directional transforms, known as contourlets which have the property of preserving edges. This paper focuses mainly on the new fingerprint compression using contourlet transform (CT), which includes elaborated repositioning algorithm for the CT coefficients, and Modified set partitioning in hierarchical trees (SPIHT) which is applied to get better quality, i.e., high peak signal to noise ratio (PSNR). The results obtained are tabulated and compared with those of the wavelet based ones.

Index Terms—Directional filter bank, Laplacian pyramid, modified SPIHT, repositioning algorithm.

I. INTRODUCTION

FINGERPRINTS are the ridge and furrow patterns on the tip of the finger and are used for personal identification of the people [1]. An automatic recognition of people based on fingerprints requires that the input fingerprint be matched with candidates within a large number of fingerprints. Since large volume of data in a database consumes more amount of memory, the information contained in fingerprints must, therefore, be compressed by extracting only visible elements, which are then encoded. The quantity of data involved is thus reduced substantially. The fundamental goal of image compression is to reduce the bit rate for transmission or storage while maintaining an acceptable fidelity or image quality. Fingerprints are digitized at a resolution of 500 pixels/inch with 256 grey levels [2]. Although there are many image compression techniques currently available, there still exists a need to develop faster and more robust algorithms adapted to fingerprints. One of the main difficulties in developing compression algorithms for fingerprints resides preserving the ridge endings and bifurcations. Compression can be achieved by transforming the data, projecting it on a basis [3] of functions, and then encoding this transform. To avoid redundancy, which hinders compression, the transform must be at least biorthogonal and in order to save

CPU time, the corresponding algorithm must be fast [3]. The two-dimensional wavelet transform satisfies these conditions. Wavelet compression allows the integration of various compression techniques into one algorithm. Recently there has been a wide interest in image representations that efficiently handle geometric structure. This comes from the recognition that wavelets essentially fail to take the advantage of geometric regularity, a common feature in natural images. In 1-D however, wavelets are known to be optimal in approximating piecewise smooth signals, a feature that is attained by the presence of vanishing moments in the transform. It is thus natural to ask the question of which equivalent feature would be responsible for an optimal approximation of piecewise smooth images. The contourlet transform [4] is proposed as a mean to fix the failure of wavelets in handling geometry by the presence of directional vanishing moments in the contourlet frame element. As fingerprints mostly contain contoured edges, the transform with directional properties are needed to give better PSNR for the same compression ratio (CR) obtained using wavelet transform. The goal of this paper is the application of contourlet transform for fingerprint compression which results in superior performance compared to JPEG-2000.

This paper is organized as follows: Section II deals with the motivation for directional transforms. In Section III Contourlet transform, the pyramidal decomposition and the directional decomposition are explained. Section IV describes the modified SPIHT algorithm suitable for CT, the parent, child relationship and the repositioning procedure are explained. Section V presents experiments and the results. Section VI concludes the paper.

II. MOTIVATION FOR DIRECTIONAL TRANSFORMS

The core of sparse signal representation lies at the foundation of many signal processing tasks, including compression, filtering, and feature extraction. Normal interest is on the construction of sparse expansions for two-dimensional signals which are smooth and free from discontinuities across smooth curves. Such signals resemble natural images and fingerprints where discontinuities are generated by edges – referred to points in the image with sharp contrast in the intensity, whereas edges are often gathered along smooth *contours* that are created by typically smooth boundaries of physical objects [4]. For one-dimensional piecewise smooth signals, wavelets provide the right tool. However, in 2-D the commonly used separable wavelets obtained by a tensor-product of 1-D wavelets are only good at capturing the discontinuities at edge points, but do not see the smoothness along contours. Thus, more powerful schemes are needed in higher dimensions.

It is known from physiological studies [5] that the receptive fields in the visual cortex are characterized as being localized, oriented and band pass. Recently, several studies were conducted to identify the sparse components of natural image patches of small sizes. Strikingly, these sparse components resemble closely the aforementioned characteristics of the visual cortex. This result supports the hypothesis that the human visual system has been tuned so as to capture the essential information of a natural scene using a least number of visual active cells. More importantly, this result suggests that for a computational image representation to be efficient, it should be based on a *local*, *directional*, and *multi-resolution* expansion. To capture smooth contours in images, the representation should contain basis functions with variety of shapes, in particular with different aspect ratios. This is the anisotropy property. A major challenge in capturing geometry and directionality in images comes from the discrete nature of the data: the input is typically sampled images defined on rectangular grids. Because of pixelization, the notion of smooth contours on sampled images is not obvious. For these reasons, unlike other transforms that were initially developed in the continuous-domain and then discretized for sampled data, the new approach starts with a discrete-domain construction and then investigate its convergence to an expansion in the continuous-domain. This construction results in a flexible multi-resolution, local, and directional image expansion using contour segments, and thus it is named the contourlet transform [6]-[8].

III. CONTOURLET TRANSFORM

The contourlet transform is a new extension of the wavelet transform in two dimensions using multiscale and directional filter banks. The contourlet expansion is composed of basis images oriented at various directions in multiple scales, with flexible aspect ratios. With this rich set of basis images, the contourlet transform effectively capture smooth contours that are the dominant feature in natural images.

Do and Vetterli proposed the pyramidal directional filter bank (PDFB) [9], which overcomes the block-based approach of curvelet transform by a directional filter bank, applied on the whole scale also known as contourlet transform (CT).

The grouping of wavelet coefficients suggests that one can obtain a sparse image expansion by first applying a multi-scale transform and then applying a local directional transform to gather the nearby basis functions at the same scale into linear structures. In essence, first a wavelet-like transform is used for *edge (points)* detection, and then a local directional transform for *contour segments* detection. With this insight, one can construct a *double filter bank* structure (Fig. 1(a)) in which at first the Laplacian pyramid (LP) is used to capture the point discontinuities, and followed by a directional filter bank (DFB) to link point discontinuities into linear structures [10]. The overall result is an image expansion with basis images as contour segments, and thus it is named the contourlet transform. The combination of this double filter bank is named *pyramidal directional filter bank* (PDFB).
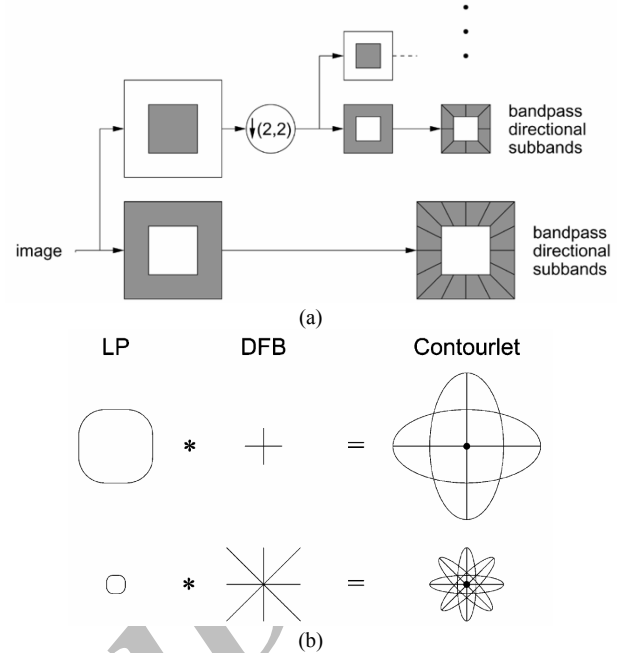

Fig. 1. (a) Block diagram of a PDFB, and (b) Supports for Contourlets.

Fig. 1(a) shows the block diagram of a PDFB. First a standard multi-scale decomposition into octave bands is computed, where the low pass channel is sub-sampled while the high pass is not. Then a directional decomposition with a DFB is applied to each high pass channel. Fig. 1(b) shows the support shapes for contourlets implemented by a PDFB that satisfies the anisotropy scaling relation. From the upper line to the lower line, the scale is reduced by four while the number of directions is doubled.

In general, the contourlet construction allows for any number of DFB decomposition levels l_j to be applied at each LP level j. For the contourlet transform to satisfy the anisotropy scaling relation, one simply needs to impose that in the PDFB, the number of directions is doubled at every other finer scale of the pyramid. Fig. 1(b) graphically depicts the supports of the basis functions generated by such a PDFB.

As can be seen from the two shown pyramidal levels, the support size of the LP is reduced by four times while the number of directions of the DFB is doubled. Combine these two steps, the support size of the PDFB basis functions are changed from one level to next in accordance with the curve scaling relation. In this contourlet scheme, each generation doubles the spatial resolution as well as the angular resolution.

The PDFB provides a frame expansion for images with frame elements like contour segments, and thus is also called the contourlet transform.

A. Laplacian Pyramid

One way of achieving a multiscale decomposition is to use a Laplacian pyramid (LP) as introduced by Burt and Adelson [11].

The LP decomposition at each step generates a sampled lowpass version of the original and the difference between the original and the prediction, resulting in a bandpass image as shown in Fig. 2(a). The process can be iterated on the coarse version.
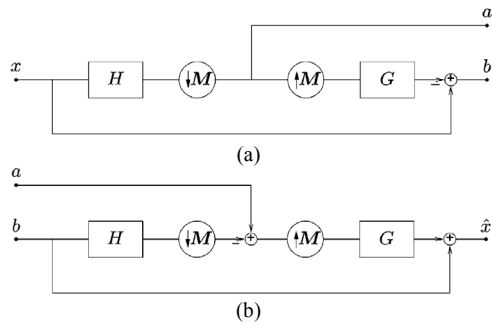
Fig. 2. Laplacian pyramid scheme (a) analysis, and (b) reconstruction.

In Fig. 2(a) the outputs are a coarse approximation 'c' and a difference 'd' between the original signal and the prediction. The process can be iterated by decomposing the coarse version repeatedly. The original image is convolved with a Gaussian kernel [7]. The resulting image is a low pass filtered version of the original image. The Laplacian is then computed as the difference between the original image and the low pass filtered image. This process is continued to obtain a set of band-pass filtered images (since each one is the difference between two levels of the Gaussian pyramid). Thus the Laplacian pyramid is a set of band pass filters. By repeating these steps several times a sequence of images, are obtained. If these images are stacked one above another, the result is a tapering pyramid data structure, as shown in Fig. 3 and hence the name.

The Laplacian pyramid can thus be used to represent images as a series of band-pass filtered images, each sampled at successively sparser densities. It is frequently used in image processing and pattern recognition tasks because of its ease of computation. A drawback of the LP is the implicit oversampling. However, in contrast to the critically sampled wavelet scheme, the LP has the distinguishing feature that each pyramid level generates only one bandpass image (even for multi-dimensional cases) which does not have "scrambled" frequencies. This frequency scrambling happens in the wavelet filter bank when a highpass channel, after downsampling, is folded back into the low frequency band, and thus its spectrum is reflected. In the LP, this effect is avoided by downsampling the lowpass channel only.

B. Directional Filter Bank

In 1992, Bamberger and Smith [12] introduced a 2-D directional filter bank (DFB) that can be maximally decimated while achieving perfect reconstruction. The directional filter bank is a critically sampled filter bank that can decompose images into any power of two's number of directions.

The DFB is efficiently implemented via a *l*-level tree-structured decomposition that leads to 2*l* subbands with wedge-shaped frequency partition as shown in Fig. 4.

The original construction of the DFB in [12] involves modulating the input signal and using diamond-shaped filters. Furthermore, to obtain the desired frequency partition, an involved tree expanding rule has to be followed. As a result, the frequency regions for the resulting subbands do not follow a simple ordering as shown in Fig. 4 based on the channel indices. The DFB is designed to capture the high frequency components
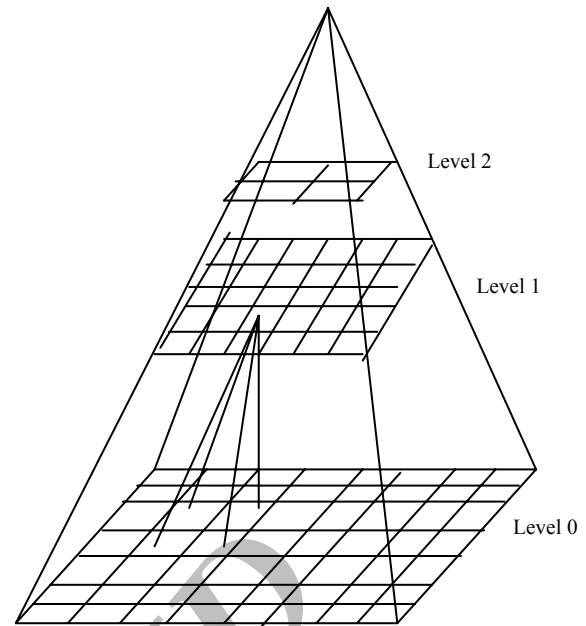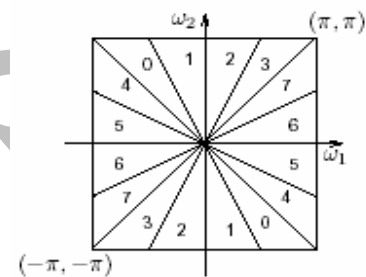

Fig. 3. Laplacian pyramid structure.

Fig. 4. DFB frequency partitioning.

(representing directionality) of images [4]. Therefore, low frequency components are handled poorly by the DFB. In fact, with the frequency partition shown in Fig. 4, low frequencies would leak into several directional subbands, hence DFB does not provide a sparse representation for images. To improve the situation, low frequencies should be removed before the DFB. This provides another reason to combine the DFB with a multiresolution scheme. Therefore, the LP permits further subband decomposition to be applied on its bandpass images. Those bandpass images can be fed into a DFB so that directional information can be captured efficiently. The scheme can be iterated repeatedly on the coarse image. The end result is a double iterated filter bank structure, named pyramidal directional filter bank (PDFB), which decomposes images into directional subbands at multiple scales. The scheme is flexible since it allows for a different number of directions at each scale.

Fig. 5 shows example contourlet transforms of the "Peppers" image. For the visual clarity, only two-scale decompositions are shown. Each image is decomposed into a lowpass subband and several bandpass directional subbands.

It can be seen that only contourlets that match with *both* location and direction of image contours produce significant coefficients. Thus, the contourlet transform effectively explores the fact image edges are localized in both location and direction.
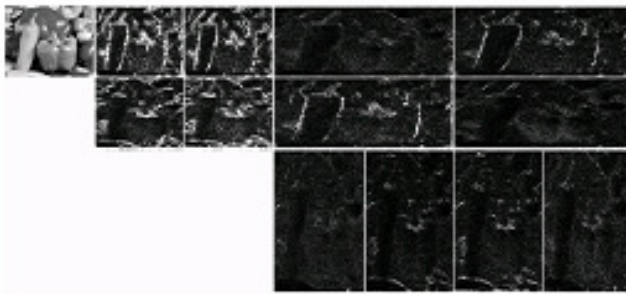
Level 2 with 4 directions   Level 1 with 8 directions

Fig. 5. Contourlet Transform of "Peppers" image.

One can decompose each scale into any arbitrary power of two's number of directions, and different scales can be decomposed into different numbers of directions. This feature makes contourlets a unique transform that can achieve a high level of flexibility in decomposition while being close to critically sampled. Other multiscale directional transforms have either a fixed number of directions or are significantly overcomplete.

With perfect reconstruction LP and DFB, the PDFB is obviously perfect reconstruction, and thus it is a frame operator for 2-D signals. The PDFB has the same redundancy as the LP: up to 33% when subsampling by two in each dimension [4], [10].

IV. MODIFIED SPIHT ALGORITHM FOR CONTOURLET TRANSFORM

In this paper, to improve the performance of the mentioned contourlet coder, it is used in conjunction with SPIHT algorithm [13] to construct an embedded image coder. Due to differences in parent-child relationships between the CT coefficients and wavelet coefficients, an elaborated repositioning algorithm for the CT coefficients is developed in such a way that a *spatial orientation trees* [14] (the *zero-trees* introduced in [13]) similar to the ones used for scanning the wavelet coefficients, is obtained. The simulation results show that the proposed coder is competitive to the original SPIHT coder, especially for a category of images that have a significant amount of textures and oscillatory patterns and therefore are not "wavelet-friendly" images.

A. Parent-Child Relationship among Contourlet Transform Coefficients

Similar to the spatial orientation tree (or zero-tree) concept of wavelet coefficients in which a parent-child relationship exists along wavelet scales, one can find parent-child dependencies in other subband systems. In the case of the contourlet transform, one can assume two different parent-child relationships depending on the number of directional decompositions in the contourlet subbands [10]. If the two successive scales in which the parent and children lie have the same number of directional decompositions, then the parent and children would lie in the corresponding directional subbands; however if the scale in which the children lie has twice as many directional subbands as the scale in which the parent lies, the four children will be in two adjacent directional subbands. These two directional subbands correspond to directional subbands as the scale in which the parent lies,
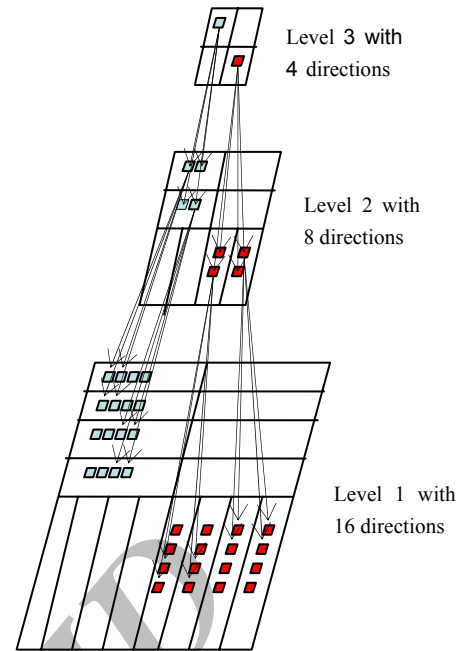

Fig. 6. Parent-child relationships in the CT.

the four children will be in two adjacent directional subbands. These two directional subbands correspond to the directional decomposition of the directional subband in which the parent is located. Fig. 6 shows the relationship when the number of directional subbands in the finer scale is twice as many as those in the coarser scale.

B. Repositioning Procedure

Due to differences in parent-children dependencies between the CT and the wavelet transform, before applying the SPIHT algorithm, the transform coefficients in the CT are repositioned in such a way to be able to use a similar SPIHT algorithm. Fig. 7 shows an example of repositioning a radial subband in the CT having 8 directional decompositions. This example assumes that the coarser subband has 4 directional decompositions. In the left image of Fig. 7, there are 8 directional subbands (separated by dashed lines).

Each two adjacent horizontal subbands (upper half subbands) and each two adjacent vertical subbands (lower half subbands) are corresponding to a horizontal subband and a vertical subband in the coarser scale, respectively. So, if the columns of the horizontal directional subbands and the rows of the vertical directional subbands are repositioned in a manner to set the children beside each other, one can benefit from using a similar tree-based wavelet coding algorithm for the CT coefficients. However, as one moves forward along the scales, the repositioning algorithm becomes more complex and one has to interlace sets of 2, 4, or any higher number of columns (rows) of the horizontal (vertical) subbands in order to maintain the descendent of a CT coefficient adjacent to each other similar to the wavelet coefficients.

Fig. 8 shows the repositioned coefficients which can now be used for application of SPIHT algorithm after making the changes in the algorithm. This repositioning groups all the children in a single scale close to each other, similar to that in wavelet transformed image matrix.
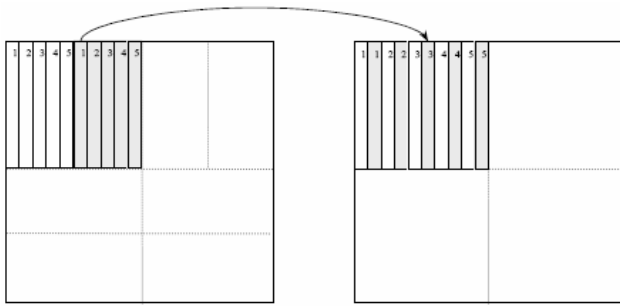
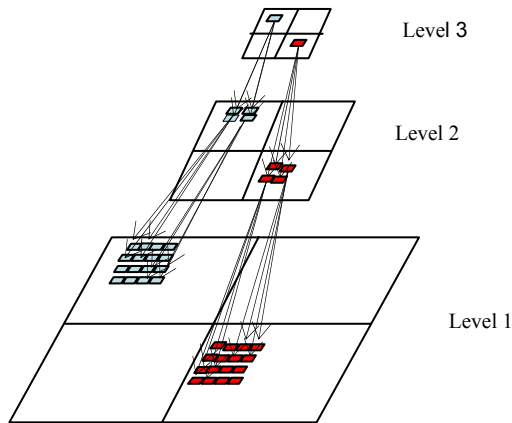Fig. 7. Example of repositioning a radial subband in the CT.

Fig. 8. Repositioning of CT coefficients.

As the scale increases, the size of the lowpass image decreases, whereas the size of the bandpass image remains same as that of the lowpass in the previous scale. Also, as the scale increases, the number of directions applied to the bandpass image decreases. In other words, the number of directions should increase from coarser scale to finer scale. This is done in order to satisfy the anisotropy scaling law.

As the scale decreases, the coefficients get more dispersed due to the increase in the number of directional sub-bands. Hence, the repositioning algorithm also gets complicated. As explained above, the repositioning is done by grouping the rows (columns) of the horizontal (vertical) sub-bands. As the scale decreases, the number of sub-bands to be considered for grouping increases, thereby, increasing the complexity of the repositioning algorithm. It can be seen that all the children of a parent are grouped near each other, similar to that of the wavelet transformed matrix. Now modified SPIHT can be applied to this matrix.

The reverse of this repositioning has to be done at the decoder side after SPIHT decoding, so that the coefficients that were grouped on the encoder side are re-distributed among the corresponding directional sub-bands. The inverse CT can be found only if this reverse procedure is done.

C. Modifications in SPIHT Algorithm

In the tree-based wavelet coding algorithms such as EZW and SPIHT, considering a threshold *T*, if a wavelet coefficient, $a(i, j)$ is *insignificant*, i.e., $a(i, j) < T$, due to a self-similarity amongst the wavelet coefficients in different subbands, it is likely that its descendents at the finer wavelet scales are insignificant. A similar observation can be made about the CT coefficients; however, the definition of the *descendants* of a CT coefficient needs to

TABLE I
PSNR AND CR FOR FINGERPRINT-A USING WT-SPIHT (FINGERPRINT-A)

Levels	Rate (bpp)	CR	PSNR(dB)
	0.2	40.00	13.90
	0.4	20.00	13.90
2	0.6	13.33	14.06
	0.8	10.00	14.06
	1	8.00	16.48
	0.2	40.00	14.02
	0.4	20.00	16.85
3	0.6	13.33	18.90
	0.8	10.00	20.46
	1	8.00	22.34
	0.2	40.00	17.09
	0.4	20.00	19.40
4	0.6	13.33	21.09
	0.8	10.00	22.69
	1	8.00	42.45

be modified. Therefore, using this presumption, and similar to the original SPIHT algorithm, a non-significant CT coefficient can be assigned to the *list of insignificant set* (LIS) and perform the same set partitioning algorithm as done within the SPIHT algorithm for wavelet coding. Hence, following the same approach of SPIHT, three sets of LIP (list of insignificant pixels), LIS, and LSP (list of significant pixels) are created and set partitioning and refining the significant pixels of the CT coefficients are done during coding.

The offspring set in wavelet based SPIHT is given by

$$O(i, j) = \{(2i, 2j); (2i, 2j + 1); (2i + 1, 2j); \quad (2i + 1, 2j + 1)\} \quad (1)$$

This is modified for CT as

$$O(i, j) = \{(i + size(M), 2j - 1); (i + size(M), 2j); \quad (i + size(M) + 1, 2j - 1); (i + size(M) + 1, 2j)\} \quad (2)$$

where *M* is the bandpass coefficient matrix in the immediately larger scale.

The H-set is initialized with the coordinates of the final lowpass coefficient matrix obtained. The other sets are same as in wavelet based SPIHT. The rest of the algorithm is unchanged. The same initializations are made on the SPIHT decoder side also.

These are the modifications needed for applying SPIHT to the Contourlet coefficients.

V. RESULTS AND DISCUSSION

Two fingerprint images are considered for the experiment (Fingerprint-A and Fingerprint-B). The images taken are of size 256×256. The PSNR results for Fingerprint-A using wavelet transform based SPIHT (WT-SPIHT) are tabulated in Table I. This WT-SPIHT comes under the standard of JPEG-2000

From the Fig. 9 it is seen that as the level of decomposition increases the value of PSNR is also increases, i.e., the hidden information available in different subbands are exploited properly giving rise to increased PSNR value. This is also evident from the rate distortion curves available in Fig. 10, which shows for the higher level of decomposition there is roughly about 15 dB increase in PSNR for the same compression ratio available at lower decomposition level. In CT-SPIHT, the
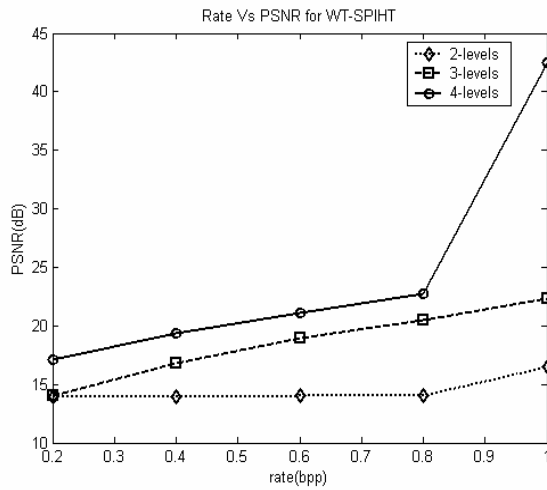
www.SID.ir

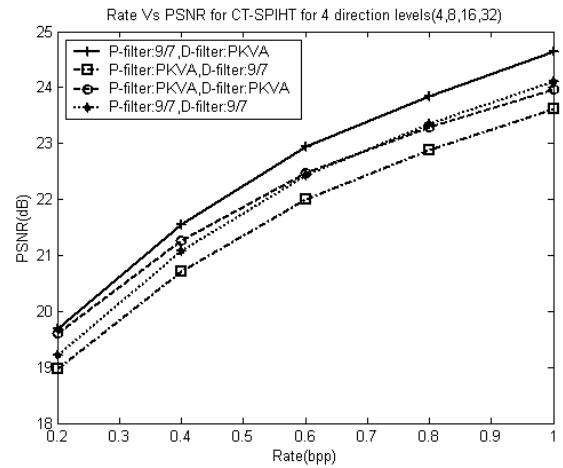Fig. 9. Rate Vs. PSNR for Fingerprint- A using WT-SPIHT.

Fig. 11. Rate vs. PSNR for Fingerprint- A using CT-SPIHT for 4 direction levels (4, 8, 16, 32).
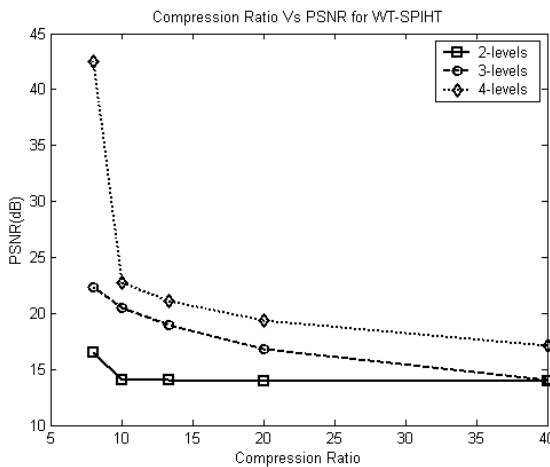

Fig. 10. Compression ratio vs. PSNR for Fingerprint-A using WT-SPIHT.
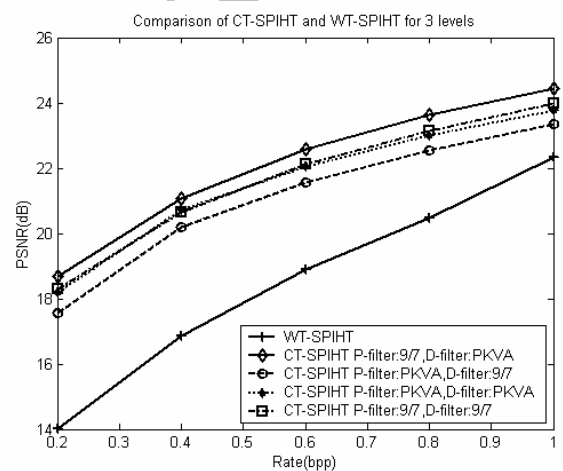

Fig. 12. Comparison of rate vs. PSNR between CT-SPIHT and WT-SPIHT for Fingerprint- A under 3 levels of decomposition.

TABLE II
PSNR VALUES FOR FINGERPRINT-A USING CT-SPIHT (CR IS SAME AS THAT OF WT-SPIHT)

Directions in each Level	Rate (bpp)	P-filter: 9/7; D-filter: PKVA	P-filter: PKVA; D-filter: 9/7	P-filter: PKVA; D-filter: PKVA	P-filter: 9/7; D-filter: 9/7
4,8	0.2	5.98	6.03	6.03	5.98
	0.4	15.48	15.58	15.58	15.48
	0.6	19.78	19.69	19.93	19.72
	0.8	21.40	20.91	21.24	21.13
	1.0	23.09	22.29	22.67	22.72
4,8,16	0.2	18.67	17.55	18.18	18.31
	0.4	21.08	20.20	20.71	20.66
	0.6	22.59	21.57	22.06	22.12
	0.8	23.63	22.56	23.01	23.15
	1.0	24.44	23.34	23.77	23.99
4,8,16, 32	0.2	19.69	18.96	19.61	19.21
	0.4	21.56	20.70	21.26	21.07
	0.6	22.94	22.00	22.47	22.43
	0.8	23.85	22.88	23.29	23.35
	1.0	24.64	23.62	23.97	24.10

Fig. 13. Comparison of Compression ratio vs. PSNR between CT-SPIHT and WT-SPIHT for Fingerprint- A under 3 levels of decomposition.

experiment consists of two stages, namely Laplacian decomposition followed by directional decomposition for the given fingerprints. The two filters chosen for the two stages of decomposition are 9/7 filter and PKVA filter. The 9/7 filter is a bi-orthogonal filter and PKVA filter is coined from the first names of the four authors who proposed it, i.e., Phoong, Kim, Vaidyanathan, and Ansari [15]. It is of quincunx/fan filters type. The different combinations between 9/7 and PKVA are tried and the corresponding
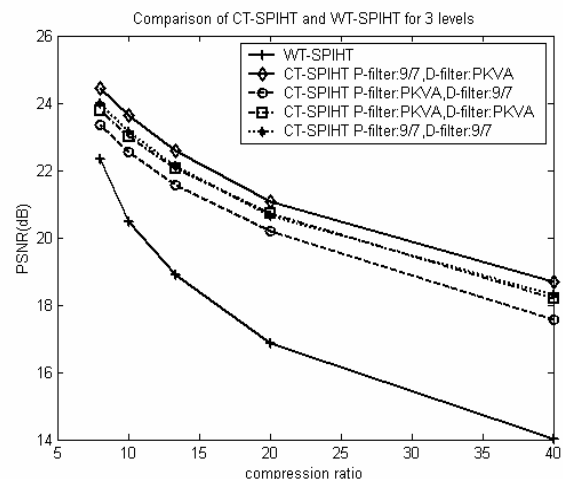
PSNR values are tabulated in Table II. It is evident from Fig. 11 that the level of directional decomposition increases the PSNR value also increases.

The results for WT-SPIHT and CT-SPIHT are compared and the comparative results are shown in Figs. 12 and 13. From these figures, it is seen that for the same compression ratio the PSNR value of CT-SPIHT is roughly 5 dB more than that of WT-SPIHT. This implies that the user can get
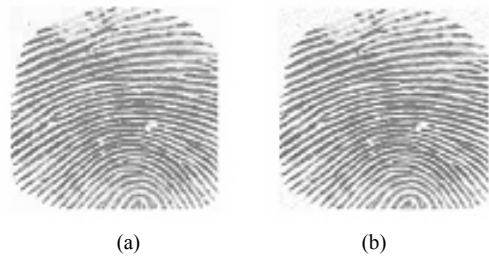
(a)   (b)

Fig. 14. Fingerprint-A reconstructed using 4 levels of decomposition for bpp=1 by (a) WT SPIHT. (b) CT- SPIHT.

TABLE III

PSNR AND CR FOR FINGERPRINT-B USING WT-SPIHT (FINGERPRINT-B)

Levels	Rate (bpp)	CR	PSNR(dB)
	0.2	40.00	10.81
	0.4	20.00	10.81
2	0.6	13.33	13.22
	0.8	10.00	13.26
	1	8.00	14.99
	0..2	40.00	12.37
	0.4	20.00	14.56
3	0.6	13.33	16.21
	0.8	10.00	17.73
	1	8.00	18.87
	0.2	40.00	14.77
	0.4	20.00	16.53
4	0.6	13.33	18.00
	0.8	10.00	19.30
	1	8.00	20.45

TABLE IV

PSNR VALUES FOR FINGERPRINT-B USING CT-SPIHT (CR IS SAME AS THAT OF WT-SPIHT)

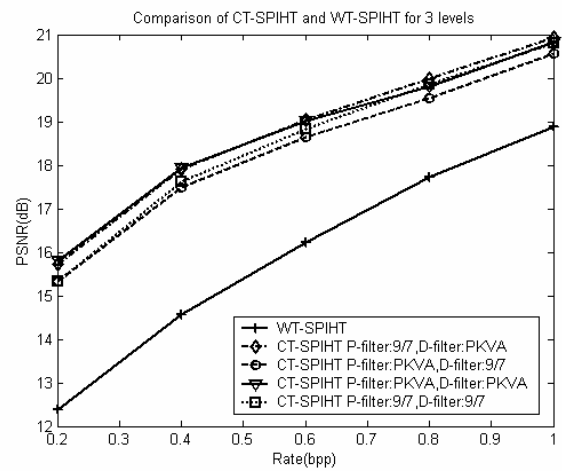| Directions in each Level	Rate (bpp)	P-filter: 9/7; D-filter: PKVA	P-filter: PKVA; D-filter: 9 /7	P-filter: PKVA; D-filter: PKVA	P-filter: 9/7; D-filter: 9/7
	0.2	6.97	6.93	6.93	6.97
	0.4	13.82	13.56	13.69	13.80
4,8	0.6	16.80	16.38	16.64	16.56
	0.8	18.60	18.31	18.56	18.37
	1.0	19.52	19.18	19.43	19.35
	0.2	15.71	15.34	15.81	15.33
	0.4	17.89	17.49	17.94	17.63
4,8,16	0.6	19.04	18.65	19.03	18.84
	0.8	19.98	19.54	19.81	19.85
	1.0	20.94	20.58	20.83	20.80
	0.2	16.42	16.01	16.39	16.09
	0.4	18.20	17.86	18.13	18.00
4,8,16, 32	0.6	19.24	18.86	19.08	19.08
	0.8	20.09	19.79	19.93	20.04
	1.0	20.96	20.69	20.83	20.90

Fig. 15. Comparison of rate vs. PSNR between CT-SPIHT and WT-SPIHT for Fingerprint-B under 3 levels of decomposition.
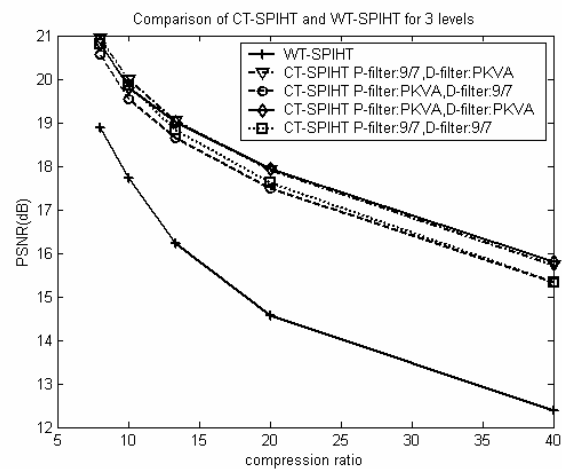

Fig. 16. Comparison of compression ratio vs. PSNR between CT-SPIHT and WT-SPIHT for Fingerprint- B under 3 levels of decomposition.

Fig. 17. Fingerprint-B reconstructed using 3 levels of decomposition for bpp=1 by (a) WT SPIHT. (b) CT- SPIHT.

extra quality of image at the reconstruction end using CT-SPIHT in comparison with WT-SPIHT.

This is achieved because of the directional basis available for CT-SPIHT not in the case of WT-SPIHT. The reconstructed Fingerprint-A using both WT-SPIHT and CT-SPIHT is shown in Fig. 14. The process is repeated for the second fingerprint, Fingerprint-B. The WT-SPIHT results are tabulated in Table III. The corresponding CT-SPIHT results are tabulated in Table IV.

From Figs. 15 and 16, once again it is seen that CT-SPIHT is superior to WT-SPIHT (JPEG-2000). The reconstructed Fingerprint-B using both WT-SPIHT and CT-SPIHT is shown in Fig. 17.

VI. CONCLUSIONS

It can be seen that the PSNR obtained by CT is higher than that of WT for the same CR. Hence, a better image reconstruction is possible with less number of bits, by using CT. Here, only four filter combinations are considered. We are currently pursuing with other filter combinations. This is a potential method for efficient fingerprint storage and transmission. As the finger prints, are mostly having higher amount of contoured and repeated patterns, CT performs superior than WT as shown in which the conducted experiments.

REFRENCES

[1]   C. H. Park, J. J. Lee, M. J. T. Smith, S. I. Park, and K. H. Park, "Directional filter bank-based fingerprint feature extraction and matching," *IEEE Trans. on Circuits and Systems for Video Technology.*, vol. 14, no. 1, pp. 74-84, Jan. 2004.

[2]   Sh. Kasaei, M. deriche, and B. Boashash., "A Novel fingerprint image compression technique using wavelet packets and pyramid lattice vector quantization," *IEEE Trans. on Image Processing*, vol. 11. no. 12, pp. 1365-1377, Dec. 2002.

[3]   K. P. Soman and K. I. Ramachandran, *Insight into Wavelets from Theory to Practice*, Prentice Hall India, New Delhi, 2002.

[4]   M. N. Do and M. Vetterli, "The contourlet transform: an efficient directional multiresolution image representation," *IEEE Trans. of Image Processing*, vol.14, no.12, pp. 2091-2106, Dec. 2004.

[5]   D. H. Hubel and T. N. Wiesel, "Receptive fields, binocular and functional architecture in the cat's visual cortex," *Journal of Physiology*, no. 160, pp. 106-154, 1962.

[6]   A. Cohen, I. Daubechies, O. Guleryuz, and M. Orchard, "On the Importance of combining wavelet-based non-linear approximation with coding strategies", *IEEE Trans. Information Theory*, vol. 48, no.7, pp. 1895-1921, Jul. 2002.

[7]   M. N. Do, *Directional Multiresolution Image Representations,* Ph.D. Thesis, EPFL, Lausanne, Switzerland, Dec. 2001.

[8]   M. N. Do and M. Vetterli, *Contourlets, in Beyond Wavelets*, Academic Press, New York, 2003.

[9]   M. N. Do and M. Vetterli, "Pyramidal directional filter banks and curvelets," in *Proc. of IEEE Int. Conf. on Image Proc.*, vol. 3, pp. 158-161, Thessaloniki, Greece, Oct. 2001.

[10] D. D. Y. Po and M. N. Do, "Directional multiscale modeling of images using the contourlet transform," *IEEE Trans. on Image Processing*, to appear, Jun. 2006.

[11] P. J. Burt and E. H. Adelson, "The Laplacian pyramid as a compact image code," *IEEE Trans. on Commun.*, vol. 31, no. 4, pp. 532-540, 1983.

[12] R. H. Bamberger and M. J. T. Smith, "A filter bank for the directional decomposition of images: theory and design," *IEEE Trans. on Signal Processing*, vol. 40, no. 4, pp. 882-893, Apr. 1992.

[13] J. M. Shapiro, "Embedded Image coding using zero trees of wavelets coefficients", *IEEE Trans. on Signal Processing*, vol. 41, no.12, pp. 3445-3462, Dec. 1993.

[14] A. Said and W. A. Pearlman, "A New fast and efficient image codec based on set partitioning in hierarchical trees", *IEEE Trans. on Circuits and Systems for Video Technology*, vol. 6, no.3 pp 243-250, Jun. 1996.

[15] S. M. Phoong, C. W. Kim, P. P. Vaidyanathan, and R. Ansari, "A new class of two-channel biorthogonal filter banks and wavelet bases", *IEEE Trans. on signal Processing*, vol. 43, no.3, pp. 649-665, Mar. 1995.

R. Sudhakar received the B.E.(Electronics and Communication Engg.) from Madras university in the year 1990 and M.E.(Communication Systems) from Thiagarajar College of Engg., Madurai in the year 2001.His research areas are: Image compression beyond Wavelets i.e., wavelet footprints, Multiwavelets, Contourlet Transform. He has published 4 papers in various International journals. He is working as Senior Lecturer in Dept. of ECE, PSG College of Technology for the past 3 years. He has nearly 12 years of teaching experience. His areas of interest include digital Signal processing, digital image processing, signals & systems, adaptive signal processing and statistical signal processing.

R. Karthiga received her B.E. (Electronics and Communication Eng.) from Sri Krishna College of Engineering and Technology. She has completed M.E (Communication Systems) from PSG College of Technology in 2005. Her areas of interest include digital image processing, wireless digital communication, wavelet transforms and statistical signal processing.

S. Jayaraman received the B.E. (Electronics and Communication Eng.) M.E and Ph.D., from PSG College of Technology. He has 28 years of teaching experience. He is currently the Professor and Head of ECE Department in PSG College of Technology. He has published more than 35 papers in Journals and Conferences. His areas of interest include DSP, Statistical Signal Processing, Multirate Signal Processing and Adaptive Signal Processing, Non linear signal processing, Multidimensional signal processing.